TETRAHEDRON GEOMETRIC FACTORS AND ACCURACY OF CURRENT DENSITY DETERMINATION

P. Robert

CNRS/CETP, F-78140 Velizy, France

ABSTRACT

The shape of the Cluster tetrahedron evolves continuously along the orbital trajectory of the spacecraft, and this shape has a major impact on the accuracy of the determination of scientific parameters related to the spatial gradient, such as the current density. A 2-D parameter is proposed to characterise the shape of the tetrahedron, based on the elongation E and the planarity P derived from the parameters of the ellipsoid defined from the volumetric tensor. The accuracy of the estimate of the current density being strongly related to the shape of the tetrahedron, we use a E-P diagram to study in detail the influence of this shape on the practical determination of J via the 4 B vectors. This is made by using many random simulated geometric configurations for the tetrahedron, and a particular isotropic magnetic structure. This simulation allow us to assess the validity of $\vec{\nabla}\cdot\vec{B}$ as a potential estimator of the accuracy of the measurement.

Key words: tetrahedron; geometry; current density; measurement errors.

1. INTRODUCTION

This paper is a summary extracted from previous work (Robert et al. 1995, Robert et al. 1998a, Robert et al. 1998b). The 2 latter correspond to chapter 13 and 16 of the ISSI book (Paschmann & Daly Eds 1998), which can be read for more details.

2. TETRAHEDRON GEOMETRIC PARAMETERS

2.1. The Volumetric Tensor

The two proposed parameters are derived from the volumetric tensor whose definition is recalled below for the special case where the origin of coordinates is chosen to be the mesocentre (C.C. Harvey 1998):

$$R_{jk} = \frac{1}{N} \sum_{\imath=1}^{N} r_{\imath j} r_{\imath k}$$

N is the number of vertices (or spacecraft) and $r_{\imath j}$ is the j component of vertex $\imath$.

The volumetric tensor being symmetric, it describes a quadratic form which can be represented by an ellipsoid in space; this ellipsoid has three principal axes, each lying in the direction of one of the eigenvectors of the tensor, with semi-length determined by the corresponding eigenvalue. If we order the eigenvalues as $R^{(1)} \geq R^{(2)} \geq R^{(3)}$ their square roots represent respectively the major, middle and minor semi-axis of the ellipsoid:

$$a = \sqrt{R^{(1)}} \qquad b = \sqrt{R^{(2)}} \qquad c = \sqrt{R^{(3)}}$$

Thus, the ellipsoide deduced from the volumetric tensor provides a simple way to visualise the global shape of a polyhedron.

2.2. Elongation and Planarity of a Polyhedron

When the polyhedron is isotropic, all three axis of the ellipsoid are equal. When it is stretched, a becomes greater than the other axis; if stretched until $b = c = 0$, all the spacecraft would lie on a straight line. When the isotropic polyhedron is squashed in one direction, c becomes smaller than the other axis; if squashed until $c = 0$, the spacecraft would lie in a plane. We define the *elongation* and the *planarity* as:

$$E = 1 - (b/a)$$

$$P = 1 - (c/b)$$

To complete the description, one can define the characteristic size as $L = 2\,a$, because this value is always non-zero. We may note that: (i) the eigenvector $\vec{R}^a$ defines the direction of elongation; (ii) the eigenvector $\vec{R}^c$ defines the normal of planarity; (iii) E and P are dimensionless, and lie in the range $0 \leq E \leq 1$, $0 \leq P \leq 1$; (iv) when $E = 1$, P is undefined because $b = c = 0$.

2.3. The Five Types of Tetrahedra

It is useful to limit the number of characteristic tetrahedra, thus we defined by means of the E and P parameters only 5 representative types of tetrahedron in the E-P plane, as shown on Figure 1. For low values of E and P we can define a "Pseudo-Sphere-shaped geometry" (bottom left corner of the E-P diagram) corresponding to the pseudo-regular tetrahedra. For a high value of P and a low value of E (top left corner of the E-P diagram) the ellipsoid is nearly a flat circle and we can define it as "Pancake-shaped". At the opposite side (bottom right corner) we can find a long ellipsoid with a pseudo-circular section, that we can define as a "Cigar-shaped". Finally, at the top right corner, we can find tetrahedra which are both elongated and flat, and we can call this type the "Knife-Blade-shaped". Note that for very elongated tetrahedron the planarity does not have much physical significance. Tetrahedra that do not belong to one of these categories or types, will be referred to "Potato type" and are located at the centre of the E-P diagram. The tetrahedra which correspond to these 5 types shown in Figure 1 are taken from a "five types reservoir" which is defined in Robert et al. 1998a.

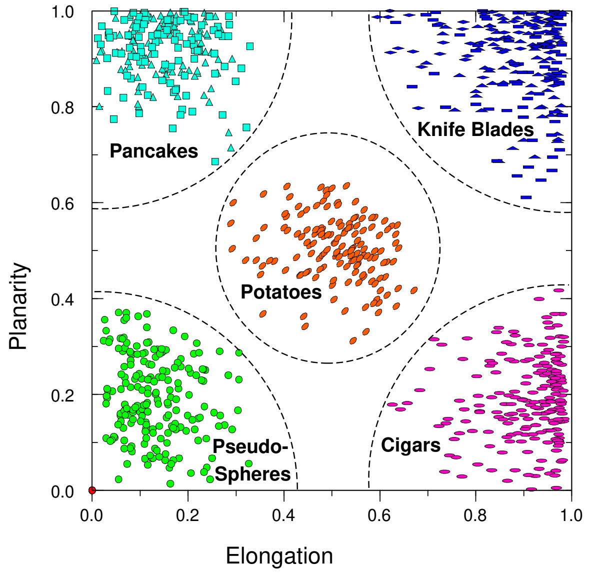

Figure 1. The five types of tetrahedra: Pseudo-Spheres, Pancakes, Cigars, Knife Blades, and Potatoes.

2.4. Cluster Orbit Tetrahedron in the E-P Diagram

The most usual representation of the orbit of 4 spacecraft is a plot of the position of each spacecraft, or other parameters, versus time. In order to characterise quickly the shape of the Cluster tetrahedron along a whole orbit, one can plot an hodogram of the successive positions of the tetrahedron in a E-P diagram, as shown in Figure 2 (December 24, 1995). The orbit has been given by ESA (J. Schœnmækers 1994b), and was established initially on the basis of a launch in November 1995. Although the launch and the Cluster mission are delayed (failure of the launch of Arianne 501), the arguments remain about the same. The time step is 6 minutes, and the arrow indicates the direction of the motion. The apogee corresponds to the portion of the figure where the different points are very close together, the velocity being low and the shape slowly varying. The perigee corresponds to the portion of the figure where the points are widely spaced, because the spacecraft velocity along the average trajectory is large.

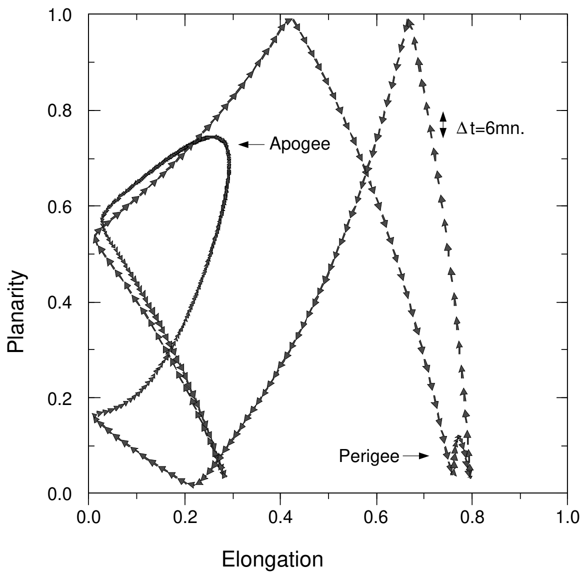

Figure 2. Evolution of the shape of the Cluster tetrahedron along its trajectory in a E-P diagram for December 24, 1995 (data provided by ESA).

The tetrahedron is regular during 2 short period along the orbit, of course these correspond to the Pseudo-Spheres type. During the rest of the curve, the E-P parameters can take extreme values. In particular the tetrahedron is absolutely flat (P=0.99) for 2 points along the orbit, but never completely linear (the maximum value of E is 0.8 near the perigee). This kind of figure can give a good indication on the shape of the Cluster tetrahedron during the orbit of the four spacecraft, which can cover all the E-P plane.

3. ACCURACY OF CURRENT DENSITY DETERMINATION

The goal is to use a simulation which allow to produce simulated data of the Cluster magnetometers, having defined a current structure model. By using many possible shapes of tetrahedra, we study the influence of the shape on the estimate of J, since the difference $\Delta J/J$ between the model and the estimated values are available.

3.1. Production of Simulated data

First, we use a high number of tetrahedra, corresponding to several possible geometric configurations, taken from a "configurations reservoir". This reservoir contains about 1000 tetrahedra and offers an homogeneous coverage of the E-P plane. Their are all normalised to the same mean inter- spacecraft distance $< D >$, and their orientations are perturbed so as to have a random orientation in space.

Second, we use a model of current density structure, with a characteristic scale larger than the size of the tetrahedra, such that all the vertices of the tetrahedra are contained inside the current structure. The structure consists of a cylindrical current tube, with an homogeneous current density, or a Gaussian current density profile. Typical values are $< D >= 1000\,\mathrm{km}$, R or $\sigma = 5000\,\mathrm{km}$, $J_o = 10^{-8}\,\mathrm{amp/m^2}$. The position of the centre of each tetrahedron is translated to $-2500\,\mathrm{km}$, in order to avoid the centre of the current structure which could be a particular case.

Third, we add independent noise on the 4 spacecraft positions to simulate the uncertainties in the knowledge of S/C attitude and location. The uncertainty Δr in the knowledge of the spacecraft position is taken to be proportional to $< D >$ and $\Delta r/r$ represent the relative accuracy in the determination of $\vec{r}_\alpha$. Typical values for $\Delta r/r$ are 1%, which correspond to the nominal values given by the Cluster project.

3.2. Computation of $\vec{J}$ and $\vec{\nabla} \cdot \vec{B}$

$\vec{J} = \vec{\nabla} \times \vec{B}/\mu_0$ and $\vec{\nabla} \cdot \vec{B}$ are computed from the perturbed simulated data by the barycentric coordinates method (Chanteur & Mottez 1993) which provides an estimate of the $\vec{J}$ vector which is compared to the real value given by the model. Thus the relative accuracy in the estimate of J, $\Delta J/J$, can be estimated. The definition of $\Delta J/J$ is:

$$\Delta J/J = \frac{\mu_0 \Delta J}{|\vec{\nabla} \times \vec{B}|^{\,\mathrm{model}}} = \frac{|\vec{J}^{\,\mathrm{estimated}}| - |\vec{J}^{\,\mathrm{model}}|}{|\vec{J}^{\,\mathrm{model}}|}$$

where $|\vec{J}^{\,\mathrm{model}}|$ is the mean value of the 4 $|\vec{J}_i|$ values of the model at the 4 vertices of the tetrahedron, and $|\vec{J}^{\,\mathrm{estimated}}|$ is the estimate of $|\vec{J}|$ by the barycentric method. This computation is made for all the tetrahedra taken from the reservoir defined in section 3.1., thus all the E-P plane is covered.

4. RESULTS

4.1. Influence of the Shape of the Tetrahedron on the Relative Accuracy $\Delta J/J$

Here we consider only an homogeneous current density profile, and therefore there is no error associated with the linear interpolation between the measurement made at the 4 spacecraft locations; only the uncertainties on the positions of the measurement points are taken into account($\Delta r/r = 1\%$). The main results are shown in Figure 3, where we have plotted the relative accuracy $|\Delta J/J|$ in an E-P diagram. The size and the colours of the circles indicate the values of $\Delta J/J$. Note that there is no small circle hidden behind a large one, the circles being sorted out by size before plotting.

Adopting the five types of tetrahedra defined in section 2.3., the main conclusion is that for a large fraction of the diagram, corresponding to the "Pseudo-Spheres type" and to a large fraction of the "Potatoes type", the relative error $\Delta J/J$ remains below 2%. For values of the elongation or planarity parameter larger than about 0.6, the errors reach 3% or more. For E or $P > 0.9$, which corresponds to a very long or a very flat tetrahedron, the error can reach 30% and more, especially of course when both E and P get of the order of unity. As a matter of fact, the error increases roughly with the radius $r = \sqrt{(E^2 - P^2)}$, which could be considered as a kind of degree in the degenerate tetrahedron, but this variation is not linear.

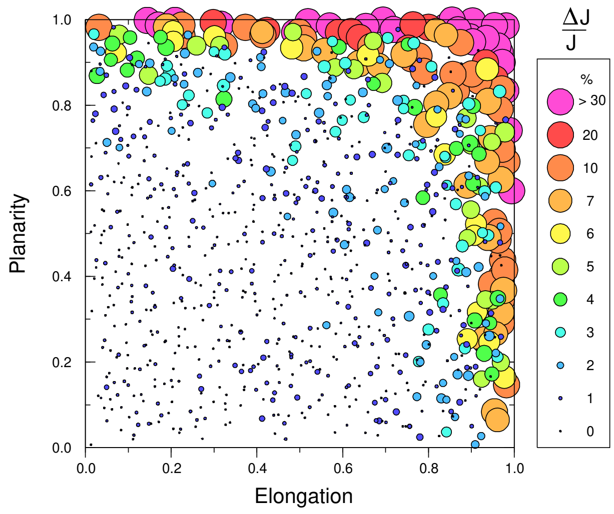

Figure 3. Influence of the shape of the tetrahedron on the estimate of the ratio $|\Delta J/J|$.

4.2. Influence of the Shape of the Tetrahedron on the Estimate of $\vec{\nabla} \cdot \vec{B}$

The theoretical value of $\vec{\nabla} \cdot \vec{B}$ is obviously equal to zero. Since $\vec{\nabla} \cdot \vec{B}$ is not a normalised quantity, we define the C_0 criterion as:

$$C_0 = \vec{\nabla} \cdot \vec{B}/|\vec{\nabla} \times \vec{B}|$$

and we use this estimated quantity rather than the value of $\vec{\nabla} \cdot \vec{B}$, to produce the Figure 4. The colour code is the same as for $\Delta J/J$. Roughly speaking, the diagram looks the same as for $\Delta J/J$, the "Pseudo-Spheres" and "Potatoes" types gives the lower values of C_0, and a large value of E or P leads to a large value of C_0.

4.3. Relationship between $\Delta J/J$ and C_0

Since the C_0 diagram looks the same as the $|\Delta J/J|$ diagram, one would expect that the criterion C_0 is an estimate of the error $\Delta J/J$. This is statistically true, but a more careful investigation shows that there is no one to one correspondence between the two diagrams; a large value of $\Delta J/J$ can correspond to a small value of C_0, and *vice versa* : good estimates of J can correspond to large value of the divergence. This is particularly true for large values of E or P.

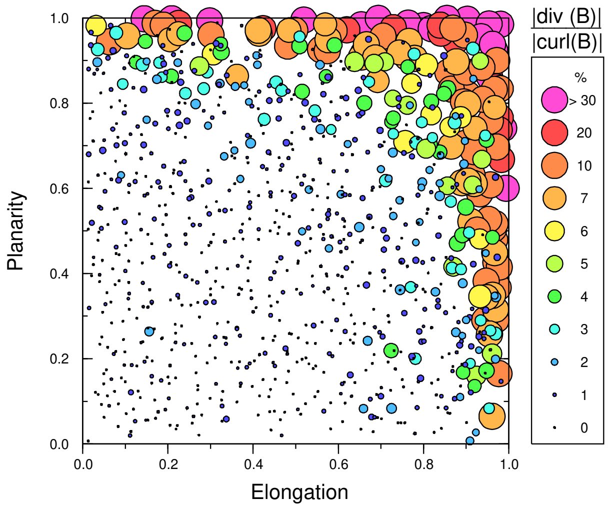

Figure 4. Influence of the shape of the tetrahedron on the criterion $C_0 = |\vec{\nabla} \cdot \vec{B}| / |\vec{\nabla} \times \vec{B}|$.

In order to reveal a possible relationship between $\Delta J/J$ and C_0, we have plotted these quantities in together in Figure 5. The colour code and the symbols correspond to the family of the tetrahedra defined in section 2.3.. A relationship between these two parameter would result in the alignment of the representative points. This is not observed; the distribution of the points has no preferred direction. Of course the area of the "Pseudo-Spheres" (round symbols) is restricted to the central part of the diagram, close to zero, while the other types cover all the diagram. The non-existence of a correlation between $\vec{\nabla} \cdot \vec{B}$ and ΔJ can be explained by the fact that the divergence is obtained from the diagonal terms of the dyadic $\vec{\nabla}\vec{B}$, while the curl is built from the off-diagonal terms. These terms being perturbed by the addition of an independent random noise, the corresponding errors on the gradient tensor are not dependent. Practically, if the errors on the various components are effectively independent, *it means that we cannot use the value of the estimated divergence to estimate the error* ΔJ *due to the measurement uncertainties.*

4.4. Influence of the Current Direction on the Error $\Delta J/J$

The possible influence of the direction of the current with respect to the largest face of the tetrahedron on the errors is investigated. Figure 6 shows the result: the relative error $\Delta J/J$ is plotted versus the angle θ between the direction of the current and the normal to the main plane of the tetrahedron (the semi-minor axis). The "Pseudo-Spheres" have been removed from the because the main plane has no meaning for a sphere. One could expect to find in this diagram a relationship between $\Delta J/J$ and θ, showing for instance that the quality of the estimate would be better when the current is orthogonal to the main plane. Examination of Figure 6 show that the (expected) minimum of $\Delta J/J$ for $\theta = 0\,\mathrm{deg}$ or $\theta = 180\,\mathrm{deg}$ seems roughly clear. One can observe a slight tendency in the case of the "Pancakes", for

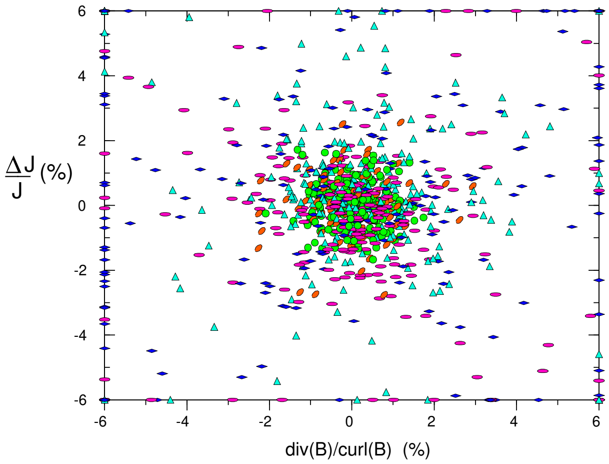

Figure 5. Relationship between the error $\Delta J/J$ *and the criterion* C_0.

which the main plane has of course the clearest meaning, but this relationship is not very obvious. Therefore, it seems that the angle θ plays a role in the organisation of the diagram, and that the error $\Delta J/J$ can be related to this angle.

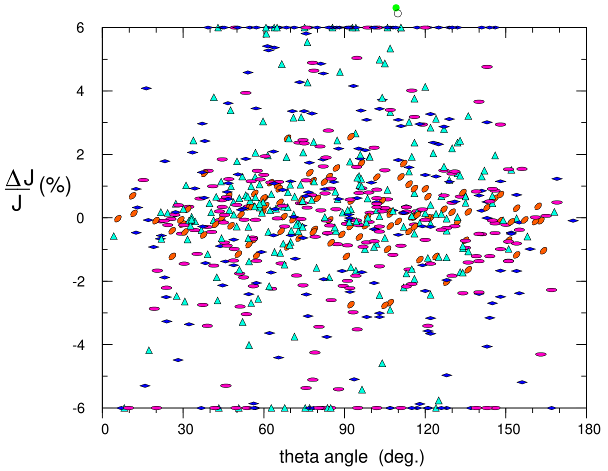

Figure 6. Influence of the current density direction on the error $\Delta J/J$.

5. CONCLUSIONS

To characterise the shape of the tetrahedron, and its orientation in space, we use the elongation and planarity parameters (E, P) computed from the ellipsoid deduced from the volumetric tensor, and the vectors $\vec{a}$ and $\vec{c}$ are used for the direction of the Elongation and the normal to the Planarity. By introducing the E-P diagram to plot quantities such as the relative accuracy $\Delta J/J$, we have a good tool to analyse the relationship between a scientific parameter and the shape of the tetrahedron, for a given event model. In the same manner, by using the θ angle between the $\vec{c}$ vector and the direction of the current, we can analyse the effect of the orientation of the tetrahedron on the accuracy of the measurement.

The relationship between the shape of the tetrahedron and $\Delta J/J$ has been shown by a simulation of the crossing, by 4 spacecraft, of a particular current density structure. The simulation gives the relative accuracy $\Delta J/J$ of the measurement plotted in an(E-P) diagram, which organises the results well and relates easily the shape of the tetrahedron to the accuracy of the estimate of $\vec{J}$ or $\vec{\nabla} \cdot \vec{B}$.

A potential relationship between $\vec{\nabla} \cdot \vec{B}$ *and* ΔJ has been studied. Statistically, the ratio $\vec{\nabla} \cdot \vec{B}/|\vec{\nabla} \times \vec{B}|$ has the same behaviour as $\Delta J/J$, but on close inspection there is no one to one correspondence. One reason is obvious: since $\vec{\nabla} \cdot \vec{B}$ and $\vec{\nabla} \times \vec{B}$ are computed from different terms of the dyadic $\vec{\nabla}\vec{B}$ used by the barycentric method, and unless the errors are dependent, there is no point to point correlation between the estimated $\vec{\nabla} \cdot \vec{B}$ and the estimated $\vec{\nabla} \times \vec{B}$, then in this case $\vec{\nabla} \cdot \vec{B}$ should not be used as a reliable estimate of the accuracy of the measurement of J.

The influence of the direction of the current with respect to the orientation of the tetrahedron has been examined. The simulation shows that there exist a correlation between the direction of the current by respect to the main plane of the tetrahedron, and the accuracy of the measurement of J, but this correlation is not very large as soon as the shape of the tetrahedron is not too much degenerated.

All these conclusions, of course, could be modified for another type of magnetic structure. The effect of different characteristic magnetic properties on measurement performance needs to be investigated more thoroughly, particularly with regard to anisotropic structure. Tools and simulations used in this paper are well suited for such an event study and should be performed in conjunction with other possible methods.

ACKNOWLEDGMENTS

The author thanks gracefully G. Chanteur for having provided the Fortran code source of the barycentric method, and J. Schœnmækers for having provided the code source of the computation of the ellipsoide, and the orbit files of Cluster I.

REFERENCES

G. Chanteur and F. Mottez. Geometrical tools for Cluster data analysis. In *Proc. International Conf. "Spatio-Temporal Analysis for Resolving plasma Turbulence (START)", Aussois, 31 Jan. 31–5 Feb. 1993*, ESA WPP–047, pages 341–344. European Space Agency, Paris, France, 1993.

C.C. Harvey. Spatial Gradients and the Volumetric Tensor. In *Analysis Methods for Multi-Spacecraft Data*, Edited by G. Paschmann and P. Daly, ISSI Scientific Report, ESA Publication Division, 1998, pages 307-322.

G. Paschmann and P. Daly (Eds). Analysis Methods for Multi-Spacecraft Data. ISSI Scientific Report, ESA Publication Division, 1998.

P. Robert, A. Roux, and G. Chanteur. Accuracy of the determination of the current density via four satellites. In *Abstracts*, Boulder, Colorado, July 1995. International Union of Geodesy and Geophysics, XXI General Assembly. Presentation GAB51H-06.

P. Robert, A. Roux, C. Harvey, M. Dunlop, P. Daly, K.H. Glassmeier. Tetrahedron Geometric Factors. In *Analysis Methods for Multi-Spacecraft Data*, Edited by G. Paschmann and P. Daly, ISSI Scientific Report, ESA Publication Division, pages 323-348, 1998a.

P. Robert, M. Dunlop, A. Roux, G. Chanteur. Accuracy of Current Density determination. In *Analysis Methods for Multi-Spacecraft Data*, Edited by G. Paschmann and P. Daly, ISSI Scientific Report, ESA Publication Division, pages 395-418, 1998b.

J. Schœnmækers. Assessment of CLUSTER constellation geometry. ESA/ESOC/ECD/OAD, private communication, 1994.

J. Schœnmækers. Cluster orbit files and software. ESA/ESOC/ECD/OAD, private communication, 1994.